# Electrostatic properties in zeolite-type materials from high-resolution x-ray diffraction: The case of natrolite

N. E. Ghermani, C. Lecomte,* and Y. Dusausoy
*Laboratoire de Cristallographie et Modélisation des Matériaux Minéraux et Biologiques, LCM³B, URA CNRS 809, Université Henri Poincaré, Nancy 1, Boîte Postale 239 Faculté des Sciences, Boulevard des Aiguillettes, 54506 Vandoeuvre-lès-Nancy Cedex, France*
(Received 16 May 1995)

High-resolution x-ray-diffraction data of natrolite at room temperature give by multipolar refinement an analytical expression of the electron density which permits the calculation of net atomic charges and electrostatic potential. The observed net charges show that the structural formula of natrolite may be written $Na_2Al_2Si_2O_8(SiO_2),2H_2O$. The electrostatic energy of one sodium ion inside the crystal is estimated to $-21.6$ eV. Calculation of the electrostatic potential excluding one sodium shows that the minimum is precisely at the removed Na position.

## I. INTRODUCTION

Zeolite materials are widely used in industry to trap cations or molecules depending on the electrostatic potential inside their cavities. If the size of the cavity as well as the crystal structure are known from conventional x-ray diffraction, nowadays, no theoretical method is able to precisely describe or reproduce the net atomic charges and the electrostatic potential in these materials. The only possibility to estimate the electrostatic properties of zeolite-type materials is high-resolution x-ray diffraction, which permits electron-density modeling and therefore calculation of the properties; we have applied this technique mainly to organic and organometallic compounds (no extinction, few absorption problems) and it is now necessary to test the feasibility of such methods on hard insulator materials. Therefore we have chosen a natural ordered zeolite (natrolite) to show that reliable atomic net charges and electrostatic potential can be obtained from a careful x-ray-diffraction study.

Since Pauling[1] in 1930, many authors have been interested in natrolite ($Na_2Al_2Si_3O_{10},2H_2O$) crystal studies. Among the zeolitic compounds, natrolite is fibrous and presents channels along the $c$ axis instead of cavities. The framework of this crystal is composed of $SiO_4$ and $AlO_4$ tetrahedra forming a helicoidal channel in which Na cations and water molecules lie on zigzag lines parallel to the $c$ axis. The full description of the ordered Si/Al natrolite structure was given initially by Pauling[1] and Taylor, Meek, and Jackson.[2] Meir[3] refined the atomic positions. From the electron-density and electrostatic-potential point of view, natrolite offers the opportunity to determine the partial covalent character of Si-O and Al-O bonds. A recent paper of Stuckenschmidt, Joswig, and Baur[4] reported the study of the deformation electron density of natrolite by the X-X method to a resolution of $(\sin\theta/\lambda)_{max}=0.9$ Å$^{-1}$. However, these authors did not use any multipolar refinement[5] to get reliable structure-factors phases for electron-density mapping nor derive any electrostatic property. In the present study, after a reliable multipolar refinement,[5] we used a $\kappa$ refinement[6] to get experimental atomic charges which permit one to map out the electrostatic potential in the crystal using a combination of Fourier and direct space summations.

## II. EXPERIMENTAL DETAILS

### A. Microprobe analysis and x-ray-diffraction experiment

A crystal of natrolite has been chosen for its well-ordered Al,Si distribution in the framework reflected by the high $b$-$a$ parameters difference.[7] The crystal structure of such a compound originating from Marienberg (Usti and Labem, CR), considered as a maximum natrolite ($b-a=0.351$ Å) has been published by Kirfel, Orthen, and Will.[8] The sample used in the present study originates from the same deposit. Among a lot of twinned crystals drawn from a geode, a single specimen was selected for its good crystalline quality, displaying a (110) elongated prism ended by a pyramid. Its dimensions are $0.10\times0.16\times0.44$ mm$^3$. Microprobe chemical analysis done on five crystals from the same geode has given the same Si/Al ratio equal to 1.5 and no other cation but Na was detected. The x-ray data collection was carried out on an Enraf-Nonius CAD4 diffractometer with graphite-monochromatized Mo $K\alpha$ radiation ($\lambda=0.709\,31$ Å) at room temperature. The cell parameters were determined by least-squares fit to the optimized setting angles of 25 reflections in the range $18°\leqslant 2\theta\leqslant 46°$ ($b-a=0.343$ Å). Table I gives the experimental conditions and details. A total of 8250 reflections was measured and recorded as $\omega$-$2\theta$ profiles to a resolution of $s_{max}=(\sin\theta)/\lambda=1.1$ Å$^{-1}$ [$q_{max}=4\pi(\sin\theta)/\lambda=13.85$ Å$^{-1}$]. To improve the statistics on low-resolution reflections contributing to the valence shells and to the electrostatic potential, supplementary equivalents $(-h,-k,-l)$ and Friedel pairs $(-h,-k,-l)$ were collected. (11,11,1), (10,4,4), and (0,0,8) reflections were chosen as standards to check the variation of the intensities during the experiment and collected every 2 h. The total x-ray exposure time of the sample was 195 h.

### B. Data processing

The DREAR package of Blessing[9,10] was used for the data reduction and error analysis of the measurements. A Lorent-

 

TABLE I. Crystal data and experimental conditions.

| | |
|---|---|
| Formula | $Na_2Al_2Si_3O_{10},2H_2O$ |
| Molecular weight (g) | 3041.8 |
| Crystal system | Orthorhombic |
| Space group | $Fdd2$ |
| $a$ Å | 18.288(2) |
| $b$ Å | 18.631(2) |
| $c$ Å | 6.583(1) |
| $V$ Å$^3$ | 2242.9(5) |
| $Z$ | 8 |
| $\rho_{calc}$ (g/cm$^3$) | 2.5 |
| Temperature (°C) | 25 |
| Diffractometer | Enraf Nonius CAD4 |
| Radiation (graphite monochromator) | Mo $K\alpha$ ($\lambda=0.709\ 31$ Å) |
| Linear absorption coefficient (cm$^{-1}$) | 6.98 |
| Scan type | $\omega$-2$\theta$ |
| $(\sin\theta/\lambda)_{max}$ (Å$^{-1}$) | 1.1 |
| Reciprocal space regions | $-40\leqslant h\leqslant 40$, $-40\leqslant k\leqslant 40$ $-14\leqslant l\leqslant 14$ |
| No. of data collected | 8250 |
| No. of data used | 5191> $[I>3\sigma(I)]$ |
| $R_1,R_2,Rw$ (internal agreements) [a] | 0.0106,0.0121,0.0200 |

[a]The internal-agreement factors are defined as $R_1=\Sigma\|\|F|^2-\langle|F|^2\rangle|/\Sigma|F|^2$, $R_2=[\Sigma(|F|^2-\langle|F|^2\rangle)^2/\Sigma|F^2|^2]^{1/2}$, $R_w=[\Sigma w(|F|^2-\langle|F|^2\rangle)^2/\Sigma w(|F|^2)^2]^{1/2}$, $I=|F|^2$, and $w=1/\sigma^2(|F|^2)^2$.

zian model of the peak-width variation was applied in order to get reflection integration limits. A decay correction based on the variation of the standard reflection intensities was applied to the data. The instrumental instability coefficient $p=0.0076(6)$ was derived from the statistical study of the standard intensities and used to estimate the variance of each intensity as $\sigma^2(|F|^2)=[\sigma_c^2(|F|^2)+(p|F|^2)^2]$ where $F$ is the structure factor and $\sigma_c^2$ is calculated from the propagation of error based on counting statistics and scan angle uncertainties $[\sigma(\omega)=0.005°]$. The ABSORB program from De Titta[11] was used to correct for absorption. The absorption factor $A$ was found in the range of 0.870 to 0.930, corresponding to a maximum loss of 15% of intensity. Moreover, in order to take into account the anomalous dispersion effect, since the natrolite space group $Fdd2$ is acentric, averaging equivalent reflections was done in the $mm2$ point group leading to excellent internal agreement indices as indicated in Table I.

## III. METHODOLOGY

### A. Spherical and pseudoatom refinements

The high-order reflections were first used to estimate atomic thermal parameters and coordinates except for hydrogen atoms. We chose a cutoff of $\sin\theta/\lambda=0.9$ Å$^{-1}$ to separate core and valence-shell contributions. This strategy is commonly applied and the description is given in many electron-density studies in the literature. Consequently, we have begun the refinement by the determination of atomic coordinates and of anisotropic motion ($U^{ij}$'s) fitting the data in the range $0.9\leqslant\sin\theta/\lambda\leqslant 1.1$ Å$^{-1}$ (Table II). These parameters were kept fixed and refined only at the last cycles of the multipolar refinement with all electron-density parameters. Hydrogen atoms of the water molecule were refined isotropically with all data and the O-H distance was imposed to be 0.96 Å. The form factors of neutral atoms Si, Al, and O and ionic $Na^+$ were calculated from Clementi and Raimondi[12] wave functions. The bound atom form factor for hydrogen was from Stewart, Davidson, and Simpson.[13] Anomalous dispersion coefficients came from Cromer.[14] Table II lists the residual indices. Although the difference maps obtained, at this stage of refinement, show deformation electron density in the bonds, this density is biased by the uncertainty of the structure-factor phases. A multipolar model is then necessary to correct the form factors, taking into account the deformation of electronic clouds. The pseudoatom model of Hansen and Coppens[5] coded in the least-squares MOLLY program was used to get electron-density maps. In this model, the pseudoatom density is expressed as

TABLE II. Least-squares statistical factors. $R=\Sigma\|F_0|-K|F_c\|/\Sigma|F_0|$, $Rw=[\Sigma w(|F_0|-K|F_c|)^2/\Sigma w|F_0|^2]^{1/2}$, GOF $=[\Sigma w(|F_0|-K|F_c|)^2/n-m]^{1/2}$, $n$ is the number of refined parameters, and $m$ is the number of the data.

| Refinement no. | $\sin\theta/\lambda$ (Å$^{-1}$) | $R$ (%) | $Rw$ (%) | GOF | $n$ | $m$ | Type |
|---|---|---|---|---|---|---|---|
| 1 | $0.9<s<1.1$ | 3.91 | 4.12 | 1.25 | 85 | 1961 | spherical |
| 2 | $0.0<s<1.1$ | 2.54 | 2.89 | 1.63 | 1 | 5191 | spherical |
| 3 | $0.0<s<1.1$ | 2.16 | 2.20 | 1.27 | 238 | 5191 | multipolar |
| 4 | $0.0<s<1.1$ | 2.32 | 2.44 | 1.38 | 18 | 5191 | $\kappa$ |

$$\rho(\mathbf{r})=\rho_c(r)+P_{val}\kappa^3\rho_{val}(\kappa r)+\sum_l \kappa'^3 R_{nl}(\kappa' r)\sum_m P_{lm}y_{lm}(\theta,\phi), \quad (1)$$

where $\rho_c$ and $\rho_{val}$ are, respectively, Hartree-Fock spherical core and valence densities, $\rho_{val}$ is normalized to one electron, and $P_{val}$ is the refined valence population parameter which gives the charge transfer with respect to the number $N_{val}$ of electrons in the valence orbitals of the atom; the net charge is then $q=N_{val}-P_{val}$. The asymmetric unit is constrained to be neutral during the refinement of $P_{val}$. In the case of natrolite, the $P_{val}$ of the water molecule has been refined separately in order to respect this neutrality. The starting $P_{val}$ parameters for the five atoms of oxygen linked to Si or Al of the framework were 6.2 instead of 6 in order to take into account the charge of the sodium cation (+1) which was never refined because of the sharpness of its 4$s$ scattering factor, which would affect only very few low order data. The $y_{lm}$ are the spherical harmonic angular functions of order 1 in real form, and $R_{nl}(r)$ are Slater-type radial functions $R_{nl}(r)=N_l r^{nl}\exp(-\zeta r)$, where $N_l$ is the normalization factor. $P_{lm}$ are the multipolar population parameters and $\kappa$ and $\kappa'$ are contraction-expansion coefficients[6] for, respectively, spherical and multipolar valence densities.

In this calculation, a local atomic orthogonal axis must be assigned to each atom: these atomic local orthogonal reference axes for Si and Al have been chosen along the twofold axis of the tetrahedral (23) $T^1$ point group. For the oxygens, the $x$ axis was taken towards Si or Al. The pseudoatom ex-

TABLE III. Atomic coordinates and anisotropic thermal parameters (isotropic for H) and their standard deviations.

| | $x$ | $y$ | $y$ | $U^{11}$ | $U^{22}$ | $U^{33}$ | $U^{12}$ | $U^{13}$ | $U^{23}$ |
|---|---|---|---|---|---|---|---|---|---|
| Si1 | 0.000 00 | 0.000 00 | 0.000 00 | 0.008 00 | 0.007 82 | 0.004 28 | 0.000 00 | 0.000 00 | 0.000 43 |
| | | | | 0.000 08 | 0.000 08 | 0.000 07 | | 0.000 13 | |
| Si2 | 0.153 28 | 0.211 32 | −0.377 06 | 0.005 19 | 0.006 36 | 0.006 31 | −0.000 89 | −0.000 58 | −0.001 25 |
| | 0.000 01 | 0.000 01 | 0.000 05 | 0.000 05 | 0.000 05 | 0.000 05 | 0.000 09 | 0.000 09 | 0.000 08 |
| Al | 0.037 43 | 0.093 72 | −0.384 60 | 0.006 61 | 0.005 24 | 0.006 26 | −0.000 74 | −0.000 76 | −0.000 80 |
| | 0.000 01 | 0.000 01 | 0.000 05 | 0.000 06 | 0.000 05 | 0.000 06 | 0.000 11 | 0.000 11 | 0.000 09 |
| O1 | 0.022 72 | 0.068 49 | −0.133 88 | 0.020 98 | 0.011 47 | 0.009 43 | 0.007 07 | 0.003 54 | −0.004 82 |
| | 0.000 04 | 0.000 04 | 0.000 13 | 0.000 25 | 0.000 19 | 0.000 18 | 0.000 38 | 0.000 44 | 0.000 36 |
| O2 | 0.070 16 | 0.181 73 | −0.389 93 | 0.005 96 | 0.006 93 | 0.011 77 | −0.000 46 | −0.001 48 | −0.003 49 |
| | 0.000 03 | 0.000 03 | 0.000 11 | 0.000 13 | 0.000 13 | 0.000 17 | 0.000 29 | 0.000 30 | 0.000 22 |
| O3 | 0.098 46 | 0.035 16 | −0.499 46 | 0.011 61 | 0.009 43 | 0.016 44 | −0.012 04 | 0.000 77 | 0.004 36 |
| | 0.000 03 | 0.000 03 | 0.000 12 | 0.000 18 | 0.000 17 | 0.000 21 | 0.000 33 | 0.000 34 | 0.000 28 |
| O4 | 0.206 48 | 0.152 63 | −0.273 95 | 0.009 57 | 0.011 08 | 0.016 49 | 0.001 37 | −0.010 58 | 0.004 27 |
| | 0.000 04 | 0.000 04 | 0.000 13 | 0.000 20 | 0.000 21 | 0.000 26 | 0.000 38 | 0.000 37 | 0.000 35 |
| O5 | 0.180 19 | 0.227 30 | −0.609 84 | 0.012 12 | 0.021 78 | 0.009 53 | 0.004 67 | 0.007 16 | −0.005 69 |
| | 0.000 05 | 0.000 06 | 0.000 13 | 0.000 24 | 0.000 30 | 0.000 25 | 0.000 46 | 0.000 40 | 0.000 46 |
| Na | 0.220 77 | 0.030 73 | −0.382 39 | 0.015 94 | 0.016 35 | 0.018 47 | −0.003 50 | −0.006 12 | −0.003 19 |
| | 0.000 02 | 0.000 02 | 0.000 08 | 0.000 12 | 0.000 12 | 0.000 14 | 0.000 26 | 0.000 25 | 0.000 19 |
| Q*w* | 0.056 55 | 0.189 44 | 0.111 41 | 0.023 45 | 0.022 49 | 0.019 02 | −0.001 64 | −0.001 83 | 0.004 77 |
| | 0.000 09 | 0.000 08 | 0.000 27 | 0.000 43 | 0.000 44 | 0.000 42 | 0.000 87 | 0.000 87 | 0.000 77 |
| H1 | 0.051 75 | 0.145 76 | 0.033 00 | 0.079 42 | | | | | |
| | 0.000 00 | 0.000 00 | 0.000 00 | 0.000 06 | | | | | |
| H2 | 0.102 93 | 0.193 80 | 0.183 15 | 0.090 03 | | | | | |
| | 0.000 00 | 0.000 00 | 0.000 00 | 0.000 08 | | | | | |

pansion was extended to the hexadecapoles ($l=4$) for Si and Al, to the octupoles ($l=3$) for O including the oxygen of water, and to the dipoles ($l=1$) for H. No chemical constraints have been imposed on the asymmetric unit during the refinements since all atoms in natrolite have different environments. For Si1, at the origin, the crystallographic twofold site symmetry reduces the number of multipolar parameters. Therefore, because the $z$ local axis was chosen along the twofold axis, any spherical harmonic containing $x^{2k+1}$ and $y^{2k+1}$ where $k$ is an integer and $x,y$ relate to the Cartesian coordinates was fixed to zero. The best radial functions of Si and Al atoms were obtained by inspection of the residual maps [$n_l=6,6,6,6$ ($l=1-4$)]. $\zeta$'s were taken from Clementi and Raimondi:[12] $\zeta_{\mathrm{Si}}=3.05$ bohr$^{-1}$ and $\zeta_{\mathrm{Al}}=2.72$ bohr$^{-1}$. For O atoms, $\zeta_{\mathrm{O}}=4.5$ bohr$^{-1}$ and the multipole exponents were, respectively, $n_l=2,3,4$ up to the octupole level.

The multipolar refinements were carried out over all reflections to a resolution of $\sin\theta/\lambda=1.1$ Å$^{-1}$. Isotropic extinction was corrected and the extinction parameter $g=0.03\times10^{-4}$ indicates that natrolite is weakly affected by extinction. In contrast to quartz, where the extinction is severe, we therefore can be very confident in the Fourier calculation of the electrostatic potential. At the convergence, the atomic positions and thermal motion parameters were relaxed and refined with all multipolar parameters in the last cycles. Final residual indices are given in Table II. Inspection of Table II shows that the goodness of fit of the multipolar refinement (refinement 3), is, as expected, lower than that of the initial spherical fit (refinement 2). This difference shows that it is necessary to use aspherical form factors of the multipolar model in order to improve the phases of the structure factors. Table III lists the fractional coordinates and the final atomic anisotropic thermal parameters. $P_{\mathrm{val}}$, $P_{lm}$, $\kappa$, and $\kappa'$ parameters of the model are deposited as supplementary material. In the residual density map shown in Fig. 1, the maxima and minima do not exceed, respectively, 0.10 and $-0.15$ $e$ Å$^{-3}$ compared to a crude estimation of experimental errors:

$$\langle\sigma^2(\Delta\rho)\rangle^{1/2}=2/V\left[\sum_H\ (\sigma^2|F_{\mathrm{obs}}|)\right]^{1/2}=0.05\ \ e\ \text{Å}^{-3}$$

and

$$\langle\sigma^2_{\mathrm{res}}\rangle^{1/2}=2/V\left[\sum_H\ (K^{-1}|F_{\mathrm{obs}}|-|F_m|)^2\right]^{1/2}=0.06\ \ e\ \text{Å}^{-3}.$$

### B. $\kappa$ refinement and net atomic charges

The charge density obtained from x-ray-diffraction data is a mean thermal density in the unit cell as pointed out by Stewart and Feil.[15] With the strategy described above using high-resolution data to fit thermal parameters in the first cycles of the refinement, we have shown that the multipolar model is able to deconvolute electron density and thermal motion. However, although the multipolar parameters give information about the atomic electron-density deformation and the bonding, they are not directly useful for charge determination. The multipolar parameters have to be integrated in the real space occupied by each atom in order to get atomic moments in the sense of Buckingham.[16] Many authors such as Hirshfeld[17] and Bader and N'guyen[18] have

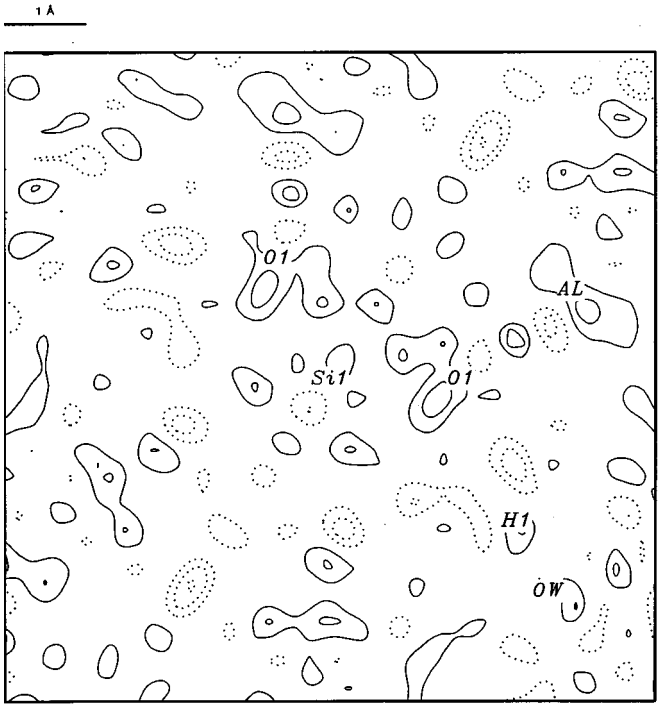


FIG. 1. Residual density in Si1-O1-Al plane of natrolite from refinement 3. Contour intervals $\pm 0.05$ $e$ Å$^{-3}$; negative contours are dashed, zero contours omitted.

looked into this molecular partitioning based on a direct space integration. On the other hand, a reciprocal space approach like the $\kappa$ refinement[6] leads to a good evaluation of the net atomic charges from x-ray-diffraction data. We have recently shown that the fit of the experimental electrostatic potential with atomic point charges[19] gives point-charge values very close to those obtained from the $\kappa$ refinement. We then calculated natrolite net charges starting from $x,y,z$ $U^{ij}$ of refinement 3, neglecting $P_{lm}$ parameters, and refining $P_{\mathrm{val}}$ and $\kappa$ only. The refinement converged very well as shown in Table II (refinement 4) and led to a significant improvement of the least-squares fit compared to the independent-atom model (IAM) refinement (refinement 2).

### C. Electrostatic potential

The knowledge of the electron-density distribution from theory or x-ray-diffraction experiments is necessary to derive the most important property to describe the interactions in the solid state, i.e., the electrostatic potential. From the Hansen-Coppens multipolar parameters we can calculate the electrostatic potential in direct space (ELECTROS program[20,21]). In molecular compounds, the electrostatic potential of an isolated molecule extracted from the crystal lattice gives information about the acid sites illustrated by the negative potential in the maps. The cohesion in such crystals is mainly due to the hydrogen bonds and many studies have shown that the electrostatic potential is more appropriate to characterize this kind of molecular interaction than electron density alone (Swaminathan and Craven[22]). But, in these materials, the molecule is an entity in itself, so the electrostatic potential around one molecule or around a little cluster of molecules is sufficient to draw conclusions about electrostatic properties. However, in inorganic materials, in order to study the electrostatic interactions, bigger clusters and lattice sums are needed. In the direct space calculations, the problem of charged boundaries appears and the method of Ewald[23] must be applied. This problem is all the more difficult when the asymmetric unit or the unit cell is polar as is the case for natrolite. To avoid this difficulty, Stewart[24] and Spackman and Stewart[25] have proposed a combination of Fourier summation and direct space lattice sums given by

$$\Phi(r)=\Delta\Phi+\Phi_{\mathrm{IAM}}+\Phi_0.$$

$\Delta\Phi$ is calculated as

$$\Delta\Phi=-\frac{1}{4\pi V}\sum_H\left[|F|\exp(i\phi_m)-|F_{\mathrm{IAM}}|\exp(i\phi_{\mathrm{IAM}})\right]\times\exp(-2\pi i\mathbf{H}\cdot\mathbf{r})/(\sin\theta/\lambda)^2, \quad (2)$$

where $V$ is the unit-cell volume, $F$ is the observed or calculated structure factor phased by $\phi_m$ from a multipolar refinement, $F_{\mathrm{IAM}}$ is the structure factor of the independent-atom model (procrystal), i.e., the superposition of spherical free atoms deduced from Hartree-Fock wave functions, and $\sin\theta/\lambda=|\mathbf{H}|/2$, $\mathbf{H}$ being the Bragg vector in reciprocal space. This $(\sin\theta/\lambda)^2$ weighting in the Fourier transform shows that $\Delta\Phi$ is less affected by series truncation errors than the electron density. The calculation of $\Delta\Phi$ in reciprocal space instead of $\Phi$ avoids the problem of the singularity at the origin when $|\mathbf{H}|$ goes to zero. On the other hand, $\Phi_{\mathrm{IAM}}$ which is the potential generated by independent atoms in direct space is rapidly convergent and does not require extensive calculations. It compensates the $F_{\mathrm{IAM}}$ term in the Fourier summation. In order to get the electrostatic potential on an absolute scale which permits one to compare the values of this quantity in one compound or another, we must also take into account the mean potential $\Phi_0$ in the crystal. This origin potential is mainly due to the quadrupolar contributions in the unit cell. It was successively estimated by Stewart,[24] Becker and Coppens,[26] and Sommer-Larsen, Kadziola, and Gajhede.[27] We have evaluated[24] $\Phi_0$ by

$$\Phi_0=-(2\pi/V)\int_{\mathrm{cell}} r^2\rho_{\mathrm{IAM}}(r)dr. \quad (3)$$

As $\rho_{\mathrm{IAM}}$ is the electron density of the independent-atom model, it is therefore not origin dependent.

## IV. RESULTS AND DISCUSSION

### A. Description of the structure

The crystal structure of natrolite has been described by several authors.[1–5] Therefore we only give a brief description necessary to understand the paper. As shown in Fig. 2, the natrolite structure contains elongated chains along the $c$ axis, composed of four-membered rings of tetrahedra in which two opposing tetrahedra are $SiO_4$ and the two others $AlO_4$. This unit is periodically reproduced along the $c$ axis by means of the $2_1$ helicoidal axis. The connecting oxygen atoms belong to two $SiO_4$ tetrahedra or to one $SiO_4$ tetrahedron and one $AlO_4$ tetrahedron. This stacking gives rise to channels in which the sodium and the water molecules are

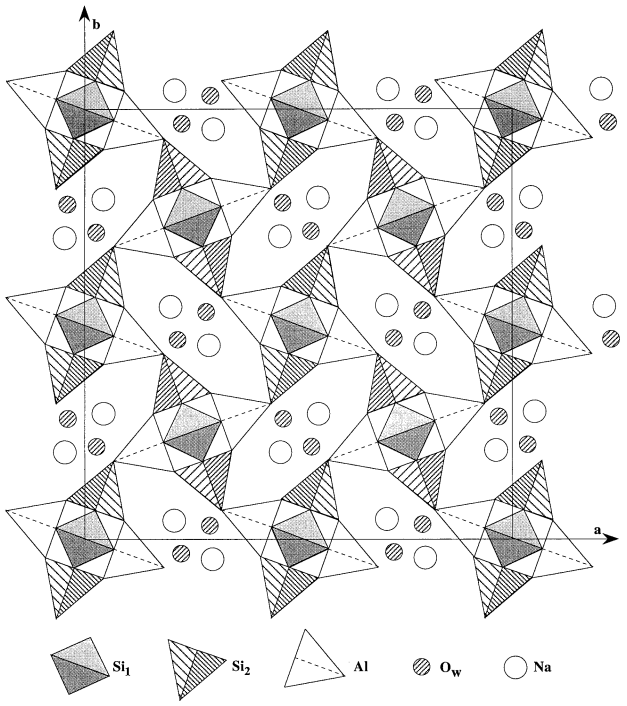


FIG. 2. View of the natrolite structure along the *c* axis.

trapped (Fig. 2). Each channel is surrounded by four other channels sharing the $O_2$ oxygen atom which bridges $SiO_4$ and $AlO_4$ tetrahedra. The sodium atoms are linked to six oxygen atoms: two water molecules and four oxygens belonging to two $SiO_4$ and two $AlO_4$ tetrahedra at two different altitudes in the channels. The comparison between the bond lengths and angles given by Kirfel, Orthen, and Will[8] after a conventional crystal structure refinement and those of the present study after the multipolar fit, shows no significant difference as reported in Table IV.

### B. Static electron density maps

Figure 3 shows the static deformation density $\Delta\rho=\Sigma_{\rm nat}[\rho^{\rm at}_{\rm mul}(\mathbf{r})-\rho^{\rm at}_{\rm IAM}]$ where $\rho^{\rm at}_{\rm mul}$ is calculated with the multipolar parameters using formula (1) and $\rho^{\rm at}_{\rm IAM}$ is the independent-atom model calculated from Clementi and Raimondi wave functions[12] (STATDENS program[20]) in the Si1-O1-Al plane, where Si1 is at the origin of the unit cell. On this map, the electron density is more concentrated around the oxygen atom than around the silicon or the aluminum according to the high electronegativity of oxygen. The peak-height values are, respectively, 0.25 $e$ Å$^{-3}$ in the Si1-O1 [Si1-O1 = 1.606(1) Å] bond and 0.45 $e$ Å$^{-3}$ in the Al-O1 [Al-O1 = 1.737(1) Å] direction at 0.5 Å from the O1 atom; the typical standard deviation of this density is 0.05–0.1 $e$ Å$^{-3}$. Even if the maxima of the electron density are not located in the middle of the bonds, electron sharing is more pronounced between Si and O enhancing a larger covalent character of the Si-O bond compare to the Al-O link. The study of electron density in ring silicates like cordierite[28] shows a similar feature in the Si-O-Al bridges. On the other hand, the electron concentration in the Si-O bond is shifted towards the interior of the O-Si-O angle and the peaks of the Si-O bonds are connected with a ridge of electron density.

TABLE IV. Interatomic distances in Å and angles in degrees in natrolite. The ESD's are given in parentheses.

| | | | |
|---|---|---|---|
| Si1-O1 | 1.6056(8) | | |
| Si1-O5 | 1.6310(9) | | |
| Si2-O2 | 1.6193(6) | Al-O1 | 1.7371(9) |
| Si2-O3 | 1.6121(7) | Al-O2 | 1.7457(6) |
| Si2-O4 | 1.6133(8) | Al-O3 | 1.7344(6) |
| Si2-O5 | 1.6368(9) | Al-O4 | 1.7430(8) |
| | | | |
| Na-O*w* | 2.371(2) | O*w*-O1 | 2.840(2) |
| Na-O*w*′ | 2.394(2) | O*w*-O5 | 3.994(2) |
| Na-O3 | 2.367(2) | H1-O1 | 1.8871(8) |
| Na-O4 | 2.3948(8) | H2-O5 | 2.0611(9) |
| Na-O2 | 2.5181(8) | | |
| Na-O2 | 2.6149(8) | | |
| | | | |
| Si1-O1-Al | 140.96(5) | O1-Si1-O1 | 113.41(6) |
| Si2-O2-Al | 129.84(4) | O1-Si1-O5 | 107.88(5) |
| Si2-O3-Al | 138.70(4) | O5-Si1-O5 | 111.09(6) |
| Si2-O4-Al | 135.00(5) | O1-Si1-O5 | 108.30(5) |
| Si1-O5-Si2 | 144.31(6) | O3-Si2-O4 | 111.78(4) |
| | | O3-Si2-O2 | 107.42(3) |
| O*w*-H1···O1 | 168.0(1) | O3-Si2-O5 | 109.79(5) |
| O*w*-H2···O5 | 160.8(1) | O4-Si2-O2 | 110.93(4) |
| | | O2-Si2-O5 | 107.16(4) |
| O3-Al-O1 | 110.10(4) | O4-Si2-O5 | 109.62(5) |
| O3-Al-O4 | 109.98(4) | | |
| O3-Al-O2 | 111.19(3) | | |
| O1-Al-O4 | 112.27(4) | | |
| O1-Al-O2 | 109.05(4) | | |
| O4-Al-O2 | 104.13(4) | | |

This feature was also reported previously by Gibbs, Downs, and Boisen[29] for coesite from theoretical calculations. In this latter paper, the deformation electron density calculated with the 6-31$G$** basis set (two $d$ orbitals on Si and one $d$ orbital on O) in $H_6Si_2O_7$ reveals a peak height of 0.35 $e$ Å$^{-3}$ in the Si-O bond which compares qualitatively with our result. The electron-density depletion around Si1 shows the silicon electron transfer to the $sp^3$ Si-O bonding orbitals. On the other hand, the water molecule oxygen lone pair shows up clearly on the map. The water molecule interacts with the O1 oxygen of the framework by means of a hydrogen bond [H1···O1=1.887(1) Å]. This feature agrees with a slight polarization of the O1 oxygen lone pairs towards H1.

### C. $\kappa$ refinement and net charges

Determining net charges of atoms in crystalline silicate-type materials is not an easy task: theoretical *ab initio* methods applied to small clusters trying to simulate the solid generally do not give a satisfactory answer because the periodicity of the crystal is not reproduced. Recently several authors have published, using the Hartree-Fock periodic program CRYSTAL,[30] the electrostatic properties such as net charges and electron density of small high-symmetry unit cells like $\alpha$-quartz[31,32] or on two-dimensional sheets of $SiO_4$ tetrahedra[33] using several basis sets with or without $d$

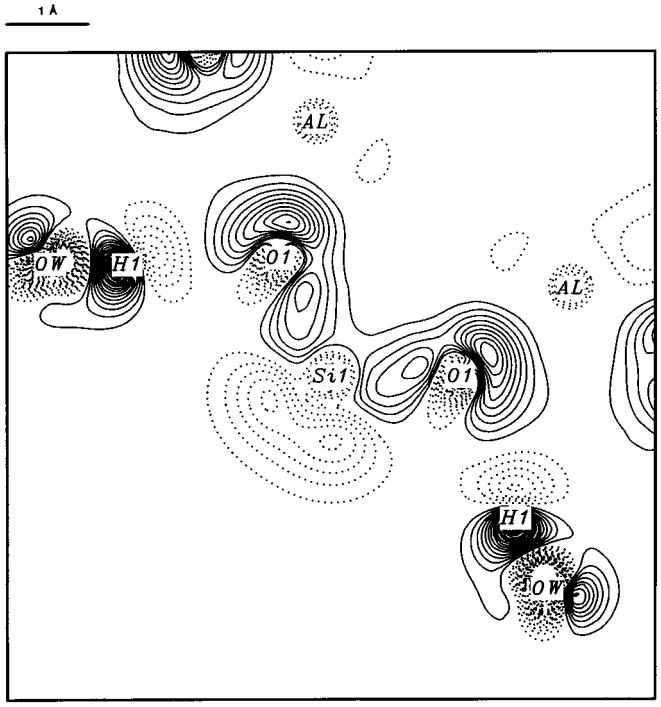


FIG. 3. Static deformation density in Si1-O1-Al plane of natrolite. Contours as in Fig. 1.

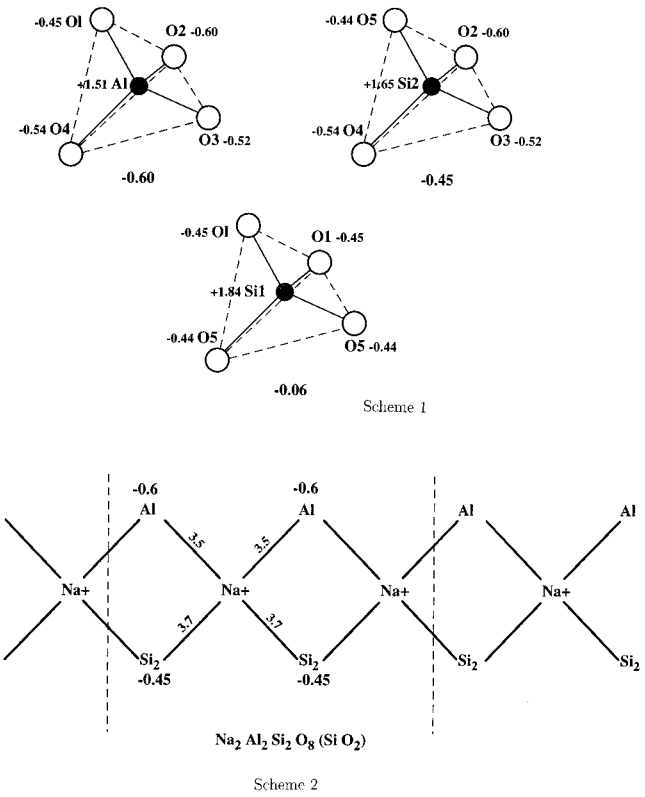


FIG. 4. Scheme 1: Global charges of Si and Al tetrahedra in natrolite. Scheme 2: Electrostatic interaction of $Na^+$ with the negative $Si(Al)O_4$ tetrahedra.

polarization functions. The charges obtained vary from 2.4 to 1.6 for the silicon atom when polarization functions are used; on quartz, the oxygen charge varies from $-1.13$ to $-0.83$, clearly showing the limit of these calculations. Anyhow, even if reliable, this type of calculation is not possible nowadays on natrolite or on real zeolites. Therefore the only way to get realistic charges in the solid state is the experimental *X-X* diffraction method especially for crystals with no severe extinction.

Table V gives $\kappa$, $P_{\mathrm{val}}$, and the net atomic charges of atoms in natrolite calculated from the $\kappa$ refinement 4. As already mentioned, the net charge of Na was kept fixed to $+1$ in all the refinements and electroneutrality imposed the sum of net charges on the framework atoms to be $-1$. The $\kappa$ values of Si1, Si2, and Al are on average 1.1 corresponding to a contraction of their electronic cloud. On the other hand, $\kappa$'s for oxygens have an average of 0.95 showing a slight expansion in agreement with Slater rules.[18] Si2 and Al bear, respectively, $1.51(11)e$ and $1.65(10)e$ net charges whereas Si1 seems to be more positively charged $[+1.84(12)e]$. The average charge value on the silicon is less than the $+2.1$ to $+2.4$ charges obtained by Sasaki *et al.*[34] on $SiO_4$ tetrahedra by direct integration of the charges in forsterite, fayalite, and tephroite; the charges in the present study are closer to those obtained by periodic *ab initio* calculations[33] on a two-dimensional sheet of $SiO_4$ tetrahedra (planar group $P31m$) using a double-$\zeta$ basis set plus polarization function including *d* orbitals on Si and reflect half ionicity of the atoms.

TABLE V. $\kappa$, $P_{\mathrm{val}}$, and net atomic charges in natrolite and their ESD's (in parentheses) from $\kappa$ refinement.

| Atom | $\kappa$ | $P_{\mathrm{val}}$ | Net charge |
|---|---|---|---|
| Si1 | 1.12(2) | 2.16(12) | 1.84(12) |
| Si2 | 1.08(2) | 2.35(10) | 1.65(10) |
| Al | 1.10(2) | 1.49(11) | 1.51(11) |
| O1 | 0.950(4) | 6.90(5) | −0.90(5) |
| O2 | 0.930(2) | 7.21(5) | −1.21(5) |
| O3 | 0.950(4) | 7.03(5) | −1.03(5) |
| O4 | 0.950(4) | 7.07(5) | −1.07(5) |
| O5 | 0.963(4) | 6.87(5) | −0.87(5) |
| Na | 1.0000 | 0.0000 | +1.0000 |
| O*w* | 0.97(2) | 6.59(3) | −0.59(3) |
| H1 | 1.17(5) | 0.76(3) | +0.24(3) |
| H2 | 1.32(7) | 0.64(3) | +0.36(3) |

The different charges obtained for Si1 and Si2 must be explained by the environment of these atoms since Si1 is bound to two silicons and two aluminums when Si2 is linked to three aluminums and one silicon. All the oxygens have obviously negative net charges. O2 is the more charged atom $[-1.21(5)e]$. It is an expected result because this oxygen atom forms ionic bonds to two Na cations in the structure [O2$\cdots$Na = 2.519(1) Å, O2$\cdots$Na′ = 2.615(1) Å]. By comparison the O1 and O5 atoms which are not directly connected to any sodium cation bear an average charge of $-0.89(5)e$. Furthermore, O3 and O4 are linked to only one $Na^+$ and have an intermediate charge of $-1.05(5)e$.

Scheme 1 in Fig. 4 gives the total charge of each of the three tetrahedra, the charges on the oxygen atoms being those obtained from $\kappa$ refinement (divided by 2 because each

oxygen atom is linked to two Si or Al ions). The Si1 tetrahedron is almost neutral, slightly positive, and therefore does not participate in the charge transfer in natrolite; in contrast, the Al and Si2 tetrahedra bear on average $-0.5(1)$ negative global charge compensating the $Na^+$ cation charge. This latter result explains the coordination of the sodium cation: as shown on scheme 2 in Fig. 4, the Na closest neighbors are the Al and Si2 tetrahedra [Na-Si2=3.068(1) Å, Na-Al= 3.101(1) Å] whereas the shortest Na$\cdots$Si1 is 4.792(1) Å showing that Si1 is more involved in the framework structure building and not in the interaction with the cations. Therefore the structural formula of natrolite should be written $Na_2Al_2Si_2O_8(SiO_2),2H_2O$ where $SiO_2$ relates to Si1. The charges obtained for the oxygen and hydrogen of the water molecule are very close to those that we got from a joint x-ray and neutron *X-N* diffraction study of *L*-arginine monophosphate, a material with nonlinear optical properties.[35]

### D. Electrostatic potential

The following strategy for mapping out the electrostatic potential in the natrolite structure is a combination of Fourier synthesis and direct space neutral-atom summations [formula (2)]. The structure factors used in these calculations were those of the $\kappa$ electron-density model (Table II, refinement 4) corresponding to the observed data $(\sin\theta/\lambda)_{max}=1.1$ Å$^{-1}$. Even if the thermal motion is present in the structure factors, we have checked, according to Stewart[24] that the electrostatic potential outside the atomic positions is not affected. One of the goals of this study was to evaluate the electrostatic energy of the $Na^+$ cations in the crystal of natrolite, so we focus on the Na sites in the structure. The mean electrostatic potential [formula (3)] found for this structure from the procrystal is $\phi_0=-0.76$ *e* Å$^{-1}$ (1 *e* Å$^{-1}$=14.4 V). For comparison, $\phi_0$ is equal to $-1.04$ *e* Å$^{-1}$ in danburite[36] and even higher in stishovite,[37] $-1.38$ *e* Å$^{-1}$. According to O'Keefe and Spence[38] these calculated values are slightly overestimated in comparison with experimental values obtained by electron-diffraction interferometry,[39] for example. Figure 5 displays the total electrostatic potential in the plane containing the zigzag line of Na (parallel to *c* axis). The electrostatic potential on this map shows minima of $-0.9$ *e* Å$^{-1}=-13.5$ V which are close to the cation positions. These negative potentials form complementary zigzag lines to those of sodium. This negative potential is due to the $-0.76$ *e* Å$^{-1}$ inner potential to which is added $-0.1$ *e* Å$^{-1}$ provided by the Na-coordinated oxygen atoms. Figure 6 shows the Na cations in the plane containing its nearest oxygen neighbors except the two water molecules which lie on each side of the plane [O*w*-Na = 2.371(2) Å, O*w*′-Na=2.394(2) Å, O*w*-Na-O*w*′=141.56°]. Bridges of electrostatic potential originating from the sodium occur towards O3 and O4 which are the closest atoms to Na cations. The same feature was reported in an electrostatic-potential study in danburite[36] and was also observed in many electrostatic interactions like hydrogen bonds in molecular compounds. On Fig. 6, the minimum of 0.9 *e* Å$^{-1}$ is located outside the oxide ion basin and between the water oxygens.

In order to estimate the electrostatic energy of the interaction between the Na cation and the crystal, we have artificially removed one sodium from the lattice by subtracting its

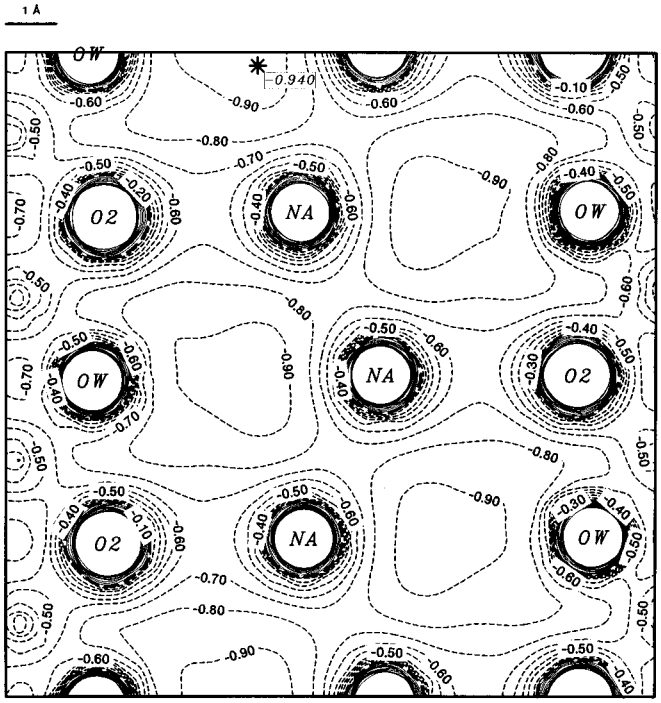


FIG. 5. Total electrostatic potential in the zigzag line of Na in the channels of natrolite. Contours are 0.10 *e* Å$^{-1}$; negative contours are dashed, zero contour dark dashed.

contribution to the total potential, assuming that the crystal is not perturbed. Figures 7 and 8 display the resulting total electrostatic potential obtained in the same planes described above. The minimum is now located exactly on the Na site and has a value of $-1.5$ *e* Å$^{-1}$ which allows one to esti-

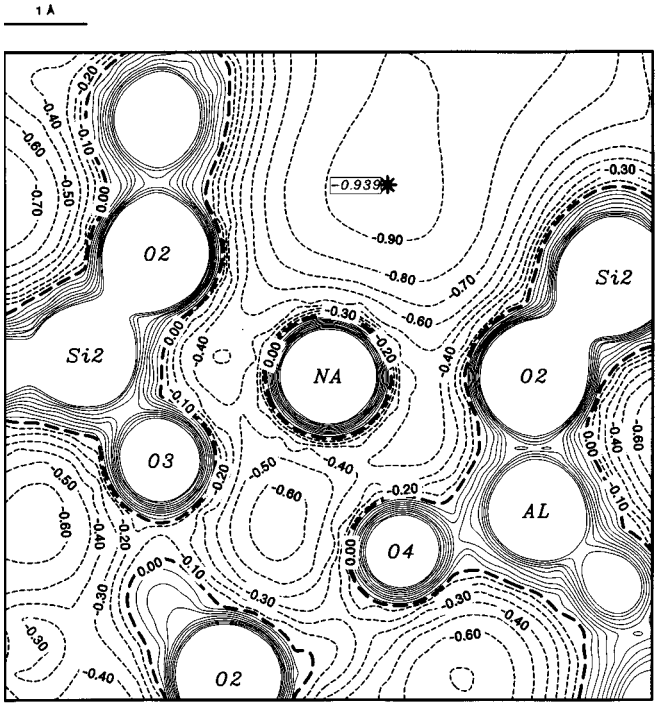


FIG. 6. Total electrostatic potential in the plane containing Na and the coordinated oxygens. Contours as Fig. 5.

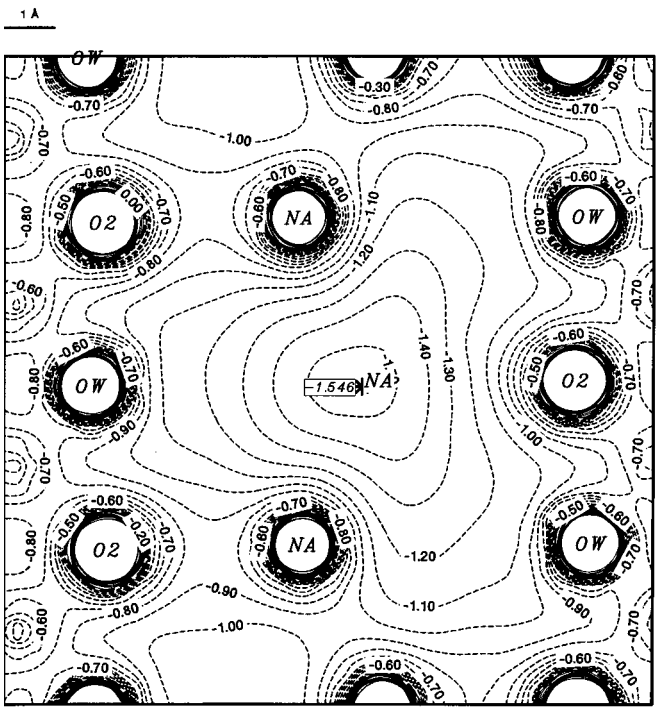


FIG. 7. Total electrostatic potential in the same plane as Fig. 5 calculated without the sodium ion. Contours as Fig. 5.

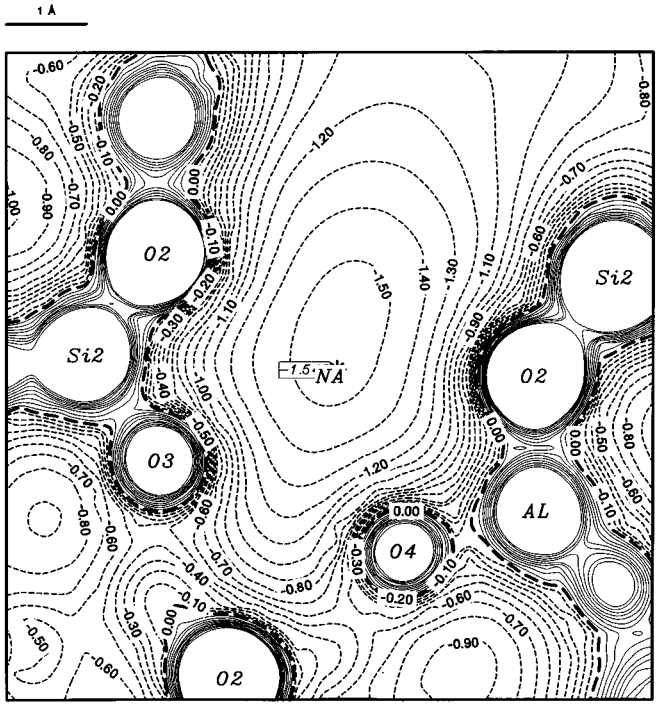


FIG. 8. Total electrostatic potential in the same plane as Fig. 6 calculated without the sodium ion. Contours as Fig. 5.

mate the electrostatic energy of the $Na^+$ ion to be $-21.6$ eV. The corresponding absolute value is much higher than the electrostatic minimum ($-0.48\ e\ Å^{-1}$) found in dehydrated zeolite *A* by Spackman and Weber,[40] showing that the $Na^+$ is more bound in the crystal of natrolite. It therefore would be interesting to have an experimental value of the Na desorption energy in natrolite or a similar compound.

## V. CONCLUSION

We have shown that reliable charges and electrostatic properties can be obtained from high-resolution x-ray-diffraction data on zeolite-type material. This type of calculation can be applied to any material for which the extinction is not a major problem. Furthermore, as synchrotron data with very short wavelengths can be collected, these calculations can be applied in the future to any material. Further work in this direction is under way. Readers interested in supplementary material related to this paper are invited to consult the PAPS[41] for multipolar parameters of natrolite.

## ACKNOWLEDGMENTS

The financial support of the CNRS, and of Université Henri Poincaré, Nancy 1 was gratefully acknowledged. The graphics have been drawn under a grant of CNI/MAT.

*Author to whom correspondence should be addressed.

[1] L. Pauling, Proc. Natl. Acad. Sci. U.S.A. **16**, 453 (1930).
[2] W. H. Taylor, C. A. Meek, and W. W. Jackson, Z. Kristallogr. **84**, 373 (1933).
[3] W. M. Meir, Z. Kristallogr. **113**, 430 (1960).
[4] E. Stuckenschmidt, W. Joswig, and W. H. Baur, Phys. Chem. Miner. **21**, 309 (1994).
[5] N. K. Hansen and P. Coppens, Acta Crystallogr. Sect. A **34**, 909 (1978).
[6] P. Coppens, T. N. Guru, P. Leung, E. D. Stevens, P. Becker, and Y. W. Yang, Acta Crystallogr. Sect. A **35**, 63 (1979).
[7] A. Alberti and G. Vezzalini, Acta Crystallogr. Sect. B **27**, 781 (1981).
[8] A. Kirfel, M. Orthen, and G. Will, Zeolites **4**, 140 (1984).
[9] R. H. Blessing, Crystallogr. Rev. **1**, 3 (1987).
[10] R. H. Blessing, J. Appl. Crystallogr. **22**, 396 (1989).
[11] G. De Titta, J. Appl. Crystallogr. **18**, 75 (1985).
[12] E. Clementi and D. L. Raimondi, J. Chem. Phys. **38**, 2686 (1963).
[13] R. F. Stewart, E. R. Davidson, and W. T. Simpson, J. Chem. Phys. **43**, 175 (1965).
[14] D. T. Cromer, in *International Tables for X-ray Crystallography*, edited by J. A. Ibers and W. E. Hamilton (Kynoch, Birmingham, England, 1974), p. 148.
[15] R. F. Stewart and D. Feil, Acta Crystallogr. Sect. A **36**, 503 (1979).
[16] A. D. Buckingham, Q. Rev. (London) **13**, 183 (1959).
[17] F. L. Hirshfeld, Theor. Chem. Acta **44**, 129 (1977).
[18] R. F. W. Bader and T. T. N'guyen, Adv. Quantum Chem. **14**, 63 (1981).
[19] N. E. Ghermani, N. Bouhmaida, and C. Lecomte, Acta Crystallogr. Sect. A **49**, 781 (1993).
[20] N. E. Ghermani, N. Bouhmaida, and C. Lecomte, ELECTROS, STATDENS, computer programs to calculate electrostatic proper-

ties from high-resolution x-ray-diffraction, CNRS URA 809, Université Henri Poincaré, Nancy 1, France.
[21] N. E. Ghermani, C. Lecomte, and N. Bouhmaida, Z. Naturforsch. Teil A **48**, 91 (1993).
[22] S. Swaminathan and B. M. Craven, Acta Crystallogr. Sect. B **40**, 511 (1984).
[23] P. P. Ewald, Ann. Phys. (Leipzig) **64**, 253 (1921).
[24] R. F. Stewart, God. Jugosl. Cent. Kristalogr. **17**, 1 (1982).
[25] M. A. Spackman and R. F. Stewart, in *Electrostatic Potentials in Crystals, Chemical Application of Atomic and Molecular Electrostatic Potentials*, edited by P. Politzer and D. G. Truhlar (Plenum, New York, 1981), p. 407.
[26] P. Becker and P. Coppens, Acta Crystallogr. Sect. A **46**, 254 (1990).
[27] P. Sommer-Larsen, A. Kadziola, and M. Gajhede, Acta Crystallogr. Sect. A **46**, 343 (1990).
[28] E. L. Belokoneva and V. G. Tsirel'son, Z. Naturforsch. Teil A **48**, 41 (1993).
[29] G. V. Gibbs, J. W. Downs, and M. B. Boisen, Jr. (private communication).
[30] R. Dovesi, C. Pisani, C. Roetti, M. Causa, and V. R. Saunders, QCPE No. 577, Indiana University, Bloomington, Indiana (1988).
[31] R. Dovesi, C. Pisani, C. Roetti, and B. Silvi, J. Chem. Phys. **86**, 6967 (1987).
[32] B. Silvi, P. D'Arco, and M. Causa, J. Chem. Phys. **93**, 7225 (1990).
[33] L. Benco and L. Smurcok, Phys. Chem. Miner. **21**, 401 (1994).
[34] S. Sasaki, K. Fujino, Y. Takénchi, and R. Sadanaga, Acta Crystallogr. Sect. A **36**, 904 (1980).
[35] E. Espinosa and C. Lecomte, (a) Ph.D. thesis, University of Barcelona, 1994; (b) (unpublished).
[36] J. W. Downs and R. J. Jeffrey Swope, Phys. Chem. **96**, 4834 (1992).
[37] M. A. Spackman, R. J. Hill, and G. V. Gibbs, Phys. Chem. Miner. **14**, 139 (1987).
[38] M. O'Keefe and J. C. H. Spence, Acta Crystallogr. Sect. A **50**, 33 (1994).
[39] J. C. Spence, Acta Crystallogr. Sect. A **49**, 231 (1993).
[40] M. A. Spackman and H. P. Weber, J. Phys. Chem. **92**, 794 (1988).
[41] See AIP document no. PAPS PRBMDO-53-5231-1 for 1 page of multipolar parameters of natrolite. Order by PAPS number and journal reference from American Institute of Physics, Physics Auxiliary Publication Service, Carolyn Gehlbach, 500 Sunnyside Boulevard, Woodbury, New York, 11 797. Fax: 516-576-2223, e-mail: janis@aip.org. The price is $1.50 for each microfiche (98 pages) or $5.00 for photocopies of up to 30 pages, and $0.15 for each additional page over 30 pages. Airmail additional. Make checks payable to the American Institute of Physics.